# Design and development of conformational inhibitors and activity-based probes for retaining glycosidases

Beenakker, T.J.M.

# 9

# Summary and future prospects

Malfunctioning of glycosidases causes various complex pathologies in man. Activity-Based Protein Profiling (ABPP) is a powerful technique to selectively analyze functional proteins in their physiological surroundings. Potent and selective activity-based glycosidase probes (ABPs) could help to understand the pathological processes connected with these enzymes. The first part of this Thesis describes the design, synthesis and application of a set of ABPs for retaining α-galactosidases, β-galactosidases, α-mannosidases and β-mannosidases. The second part of this Thesis focuses on the design of functionalized bicycle [4.1.0] heptanes as potential competitive inhibitors of glycosidases (α-galactosidases, β-galactosidases, α-glucosidases and β-glucosidases) and glycosyltransferases (both galactosyltransferases and glucosyltransferases).

**Chapter 1** provides a brief overview of the basics of the ABPP technology. As well, information is provided on the reaction itineraries of retaining glycosidases, which are at the basis of the design of the covalent and competitive glycosidase inhibitors presented in this Thesis. Finally, the potencies of transition-state based inhibitors are described including therapeutic examples. **Chapter 2** describes the development and validation of α-galactosidase selective probes that may be used to study the lysosomal storage disorders (LSDs), Fabry disease and Schindler disease. Both *N*-acylated- and *N*-alkylated versions of α-galactose-configured cyclophellitol aziridines were examined on their capacity to inhibit and label, in an ABPP setting, retaining α-galactosidases. The *N*-acylated version is more prone to hydrolysis during purification and lyophilisation than its *N*-alkylated counterpart. However, this probe also proved the most effective in labeling retaining α-galactosidases.
The synthesis and validation of a new β-galactosidase selective probe is presented in **Chapter 3**. Once the synthesis of the one-step ABP using the conventional method turned out to be abortive, a two-step bioorthogonal labeling approach was attempted. In this way, the human retaining β-galactosidase, GALC (lysosomal galactocerebrosidase) could be detected in kidney lysate by in-gel labeling. In a final attempt to obtain a one-step ABP, inverse-electron-demand Diels-Alder (IEDDA) ligation was successfully applied to obtain a potent one-step β-galactosidase probe for labeling of GLB1 and GALC in mouse kidney homogenates. This probe may in turn be used as tool to study GM1 gangliosidosis, Morquio B syndrome and Krabbe disease which are caused by mutations in GH35 and GH59 galactosidases, GBL1 and GALC, respectively.
Looking forward to the sections on competitive inhibitors, Birch reduction of compound **1**[1], which featured as an intermediate in the synthesis of galactose-configured cyclophellitol, may yield cyclohexene **2** (Figure 9.1). Compound **2** may adopt the $^{4}H_{3}$ conformation and thereby mimic the oxocarbenium ion transition-state of α-galactosidases (**3)** and β-galactosidases (**4**). Therefore, compound **2** may act as a potential reversible galactosidase inhibitor.

The library of glycosidase ABPs is extended in **Chapter 4** with the synthesis and validation of ABPs for retaining α-mannosidases. The reaction itinerary of α-mannosidases is different from the previously described glycosidases, and a boat ($B_{2,5}$) transition-state conformation is expected to emerge during substrate processing. A covalent enzyme-inhibitor complex was obtained after soaking of α-mannosidase configured cyclophellitol aziridine in GH38 Golgi α-mannosidase II from drosophila.

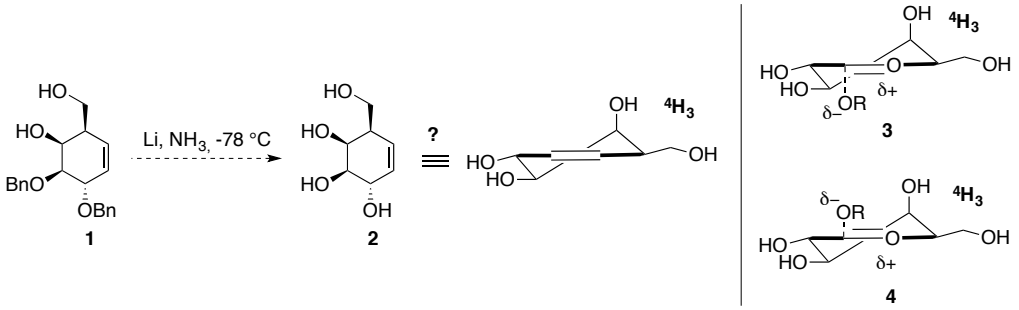


**Figure 9.1** Cyclohexene **2** may adopt the $^{4}H_{3}$ conformation and therefore conformationally mimic the oxocarbenium ion transition-state of α-galactosidases (**3**) and β-galactosidases (**4**).

Herein, the cyclohexane has adopted the skew boat ($^{1}S_{5}$) conformation as expected from the reaction itinerary. The corresponding Cy5-functionalized ABP proved to label GH38 jack bean α-mannosidase in an activity-dependent fashion. Follow-up ABPP experiments *in vitro* and *in vivo* will reveal whether the α-mannosidases probes will be of use in diagnosing α-mannosidase connected diseases such as α-mannosidosis or larynx cancer, and the identification of therapeutics aimed at correcting these diseases.[2] The first part of this Thesis ends with the description, in **Chapter 5**, of a set of GH2 exo-β-mannosidase selective ABPs. The β-mannopyranose-configured cyclophellitol aziridine based probes were validated in ABPP experiments with exo-β-mannosidases from *Helix p.* Furthermore, ABPP experiments in lysates of mice kidney resulted in labeling of MANBA, a GH2 β-mannosidase that is deficient in β-mannosidosis.

Based on the results for mannosidases presented in this Thesis, it would be of interest to develop cyclophellitol-based ABPs (**5** – **7**, Figure 9.2) for other retaining exoglycosidases for which a boat transition-state conformation is expected as part of the reaction itinerary.[3] In case of GH39 α-idurodinase, for example, such a $^{2,5}B$ transition-state is expected to occur during substrate processing.[4] α-Idurodinase selective ABPs (**5**) for ABPP would be of interest to investigate mucopolysaccharidosis

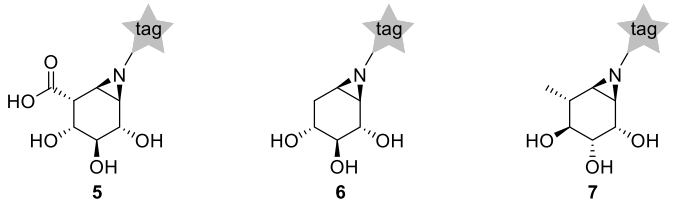


**Figure 9.2** Putative ABPs to target GH39 α-idurodinase (**5**), GH120 β-xylosidase (**6**) and GH78 α-rhamnosidase (**7**).

I, caused by α-idurodinase deficiency.[5] Another target could be GH120 β-xylosidase, found in *Bifidobacterium adolescentis*. Monitoring this enzyme with ABPs (**6**) could be of interest as this bacteria is present in the human gut.[6] Finally, GH78 α-rhamnosidase is of industrial interest as this enzyme is used in the debittering of citrus juices.[7-9] With ABPP using ABP **7** the enzyme activity could be monitored under various conditions.

A putative synthesis of the α-L-rhamnopyranose-configured cyclophellitol aziridine based ABP **7** is depicted in Scheme 9.1. The synthetic strategy is based on the synthesis of cyclophellitol as described by Madsen and co-workers[10], which has recently been

**Scheme 9.1** Synthesis of α-L-rhamnopyranose-configured cyclophellitol aziridine based ABP **7**.

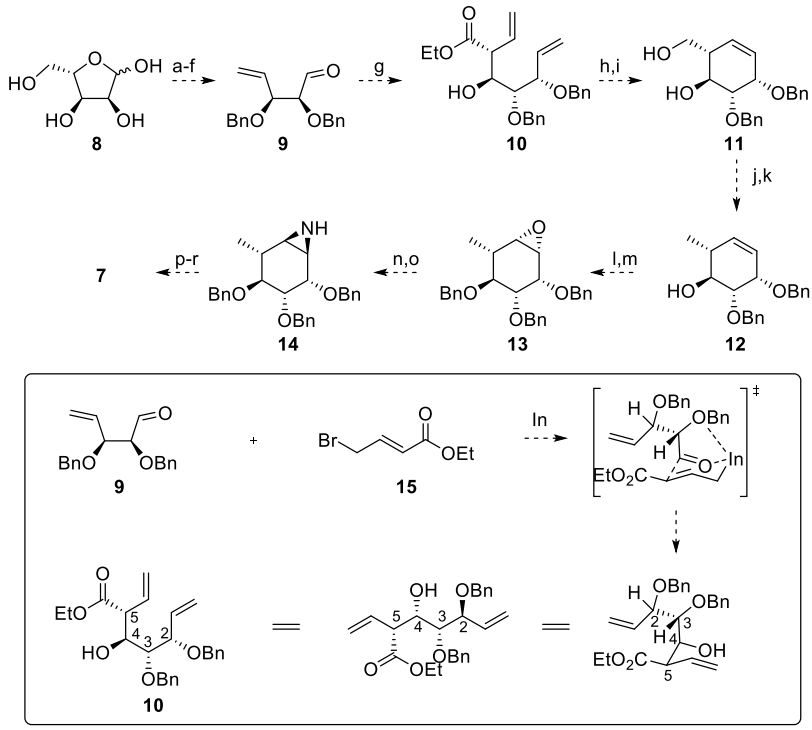


**Reagents and conditions:** a) acetyl chloride, MeOH, 0 °C to rt; b) trityl chloride, pyridine, rt; c) BnBr, NaH, DMF, 0 °C to rt; d) *p*TsOH, DCM/MeOH (1:1), rt; e) *i.* $PPh_3$, imidazole, THF, reflux; *ii.* $I_2$, THF, reflux; f) Zn, THF/$H_2O$ (9:1), 50 °C, sonicate; g) ethyl 4-bromocrotonate, In (powder), $La(OTf)_3$; h) Grubbs II, DCM, reflux; i) *i.* DIBAL, THF, 0 °C to rt; *ii.* $NaBH_4$, EtOAc/$H_2O$ (2:1); j) *p*TsCl, $Et_3N$, $CH_2Cl_2$; k) $LiAlH_4$, THF, 0 C to rt; l) BnBr, NaH, DMF, 0 °C to rt; m) *m*CPBA, DCE, reflux; n) $NaN_3$, $LiClO_4$, MeCN, 80 °C; o) $PPh_3$ polymer-bound on styrene-divinylbenzene copolymer, $CH_3CN$, reflux, overnight; p) Li, THF, $NH_3$ (l), - 60 °C; q) 1-azido-8-iodooctane, $K_2CO_3$, DMF, 80 °C, r) alkyne tags (see Chapter 4), $Cu.SO_4{\cdot}5H_2O$, sodium ascorbate, DMF, rt.

optimized.[11] Commencing with L-ribose[12] (**8**) as starting material, aldehyde **9** may be obtained in 6 steps. Subsequently the stereoselective indium-catalyzed Barbier reaction with ethyl-4-bromocrotonate may be performed to obtain compound **10**. The proposed stereoselective outcome of this reaction can be explained by the formed 6-membered transition state (Scheme 9.1). Grubbs II catalyzed ring closure metathesis of **10** followed by reduction of the ethyl ester may give compound **11**. Tosylation of the primary alcohol followed by treatment with lithium aluminium hydride[13] may afford L-rhamnopyranose-configured cyclohexene **12**. After benzylation of **12**, epoxidation with *m*CPBA may give the desired epoxide **13** and the diastereomeric isomer which may be separated by silica column chromatography. Treatment of epoxide **13** with sodium azide and lithium perchlorate[14], followed by a Staudinger reaction using triphenylphosphine on beads may yield aziridine **14**. After the Birch reduction, *N*-alkylation with 1-azido-8-iodooctane and azide-alkyne Huisgen cycloaddition with a specific alkyne-tag (see Chapter 4), ABP **7** may be obtained.

The galactopyranose-configured cyclophellitol (**16**) is an oxocarbenium ion transition-state mimic (Scheme 9.2A and B). The introduction of a sulfate group, as in compound **17**, may result in a $^4C_1$ conformational substrate mimic, which is susceptible to form a covalent enzyme-substrate adduct (Scheme 9.2C). The synthesis of this new class of cyclophellitols was explored starting from *manno*-configured cyclohexene **18** (Scheme 9.2D). Ruthenium(III)-catalyzed *syn*-dihydroxylation[15] of **18** proceeded in a stereoselective fashion and resulted into compound **19**. After treatment with thionyl chloride and subsequent ruthenium catalyzed oxidation, cyclic sulfate **20** was obtained. Palladium-catalyzed hydrogenation gave target compound **21** (TB612). The conformation of TB612 may be confirmed by DFT calculations. No inhibition of TB612 in jack bean α-mannosidase was measured up to 50 μM. This result was expected, as the $^4C_1$ conformation is not part of the reaction itinerary of α-mannosidase. The herein described synthetic strategy could be extended to α-galactopyranose-configured cyclophellitols.

In **Chapter 6** the synthesis is described of a focused library of carba-cyclophellitol based compounds with α-glucopyranose, β-glucopyranose, α-galactopyranose and β-galactopyranose configuration. These are potential reversible inhibitors for glycosidases by mimicking the transition-state conformation of the oxocarbenium ion during the reaction itinerary. Alcohol **23** and ether **25** may be added to the described library (Scheme 9.3). Debenzylation of compound **22** using palladium-catalyzed

**Scheme 9.2** Synthesis of cyclophellitol cyclosulfate **21**.

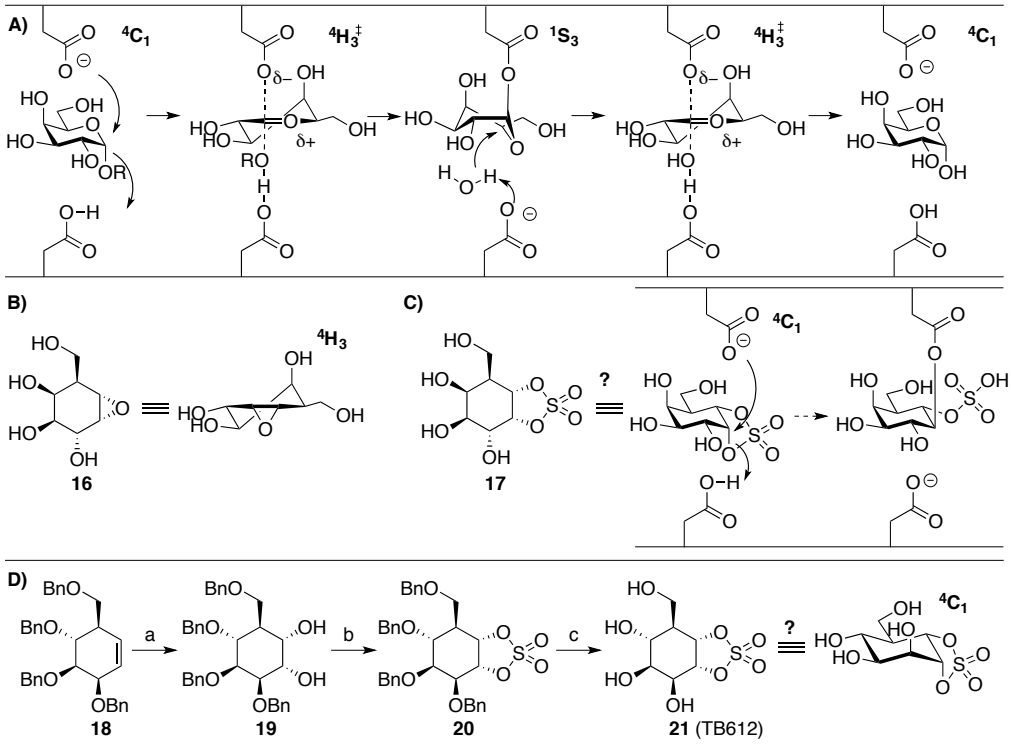


A) Proposed mechanisms of GH27 α-galactosidases. B) Galactopyranose-configured cyclophellitol (**16**) adopts a $^4H_3$ conformation and mimics the oxocarbenium ion transition-state of GH27 α-galactosidases. C) Compound **17** may adopt a $^4C_1$ conformation and mimic the substrate conformation. Reagents and conditions: a) $NaIO_4$, $RuCl_3.3H_2O$, $H_2O$, EtOAc, MeCN, 0 °C, 1 h, 68%; b) *i*) $SOCl_2$, $Et_3N$, $CH_2Cl_2$, *ii*) $NaIO_4$, $RuCl_3.3H_2O$, $H_2O$, $CCl_4$, MeCN, 0 °C, 1.5 h, 41% over 2 steps; c) 10% Pd/C, $H_2$, MeOH, 50%.

hydrogenolysis conditions may give target compound **23**. Alkylation (use of EtBr and a base) of alcohol **22**, followed by palladium-catalyzed hydrogenolysis may afford compound **25**.

**Scheme 9.3** The putative synthesis of β-glucopyranose-configured carba-cyclophellitol **23** and **25**.

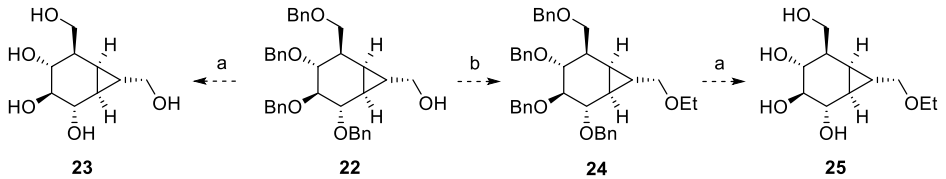


**Reagents and conditions**: a) $Pd(OH)_2/C$, $H_2$, MeOH, rt; b) EtBr, NaH, TBAI, DMF, 0 °C to rt.

The β-glucopyranose-configured carba-cyclophellitols are biologically evaluated in **Chapter 7** on their inhibitory potency of *Thermotoga maritima Tm*GH1 β –glucosidase, GBA1 and GAA. Carba-cyclophellitols turned out to be selective β-glucosidase inhibitors. Futhermore, carba-cyclophellitol (**26**) with an *N*-(4-azidobutyl)carboxamide moiety is the most potent *Tm*GH1 inhibitor ($K_i$ of 8.2 nM, Figure 9.3). Next, the conformation of the carba-cyclophellitol derivatives were analysed by $^1$H NMR analysis, quantum mechanical analysis and DFT calculations, which all supported the $^4H_3$ conformation as the preferential conformation adopted by β-glucopyranose-configured carba-cyclophellitols. After soaking of carba-cyclophellitol DW082 in *Tm*GH1, the obtained structure was analysed by X-ray crystallography, revealing that DW082 also shows up in $^4H_3$ conformation when bound to the active site of this enzyme. As various glycosidase inhibitors are in clinical use or under examination as inhibitors, probes or pharmacological chaperones, the selectivity and tight binding properties of cyclopropyl sugars may be an attractive class for further investigation. Intestinal α-glucosidases, for example, is a target for treatment of diabetes mellitus type 2. Reversible inhibitors have been approved and are applied in the clinic.[16] The α-glucopyranose-configured carba-cyclophellitols, as described in **Chapter 6**, are designed as reversible α-glucosidase inhibitors and were examined as such. However, no inhibition up to 100 uM was observed using the 4-methylumbelliferyl-α-D-glucopyranoside as substrate in α-glucosidases (GAA or GANAB). Similarly the α-galactopyranose-configured carba-cyclophellitols were examined as potential α-galactosidase inhibitors and no inhibition up to 500 uM was observed using the 4-methylumbelliferyl-α-D-galactopyranoside as substrate and α-GalA as the glycosidase. The described β-galactopyranose-configured carba-cyclophellitols, however, do inhibit β-galactosidases in the micromolar range (Figure 9.3 and Table 9.1).

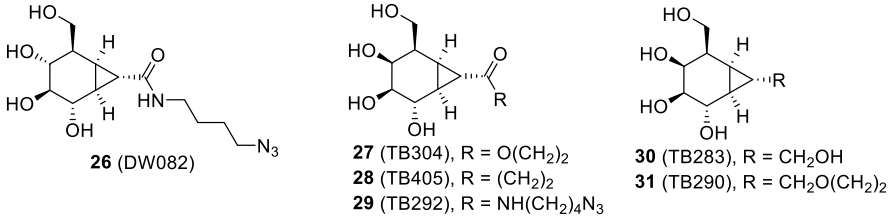


**Figure 9.3** The structures of DW082 (**26**) and β-galactopyranose configurated carba-cyclophellitols (**27** – **31**).

**Table 9.1** The apparent $IC_{50}$ values of compound **27** - **31** towards GALC and α-GalA in μM with 4-methylumbelliferyl-α-D-galactopyranoside as substrate.

| Compound | β-galactosidase (GALC) | α-galactosidase (α-GalA) |
|---|---|---|
| **27** (TB304) | >500 | >500 |
| **28** (TB405) | 205.40 ± 10.95 | >500 |
| **29** (TB292) | 39.91 ± 2.86 | >500 |
| **30** (TB283) | 76.67 ± 0.89 | >500 |
| **31** (TB290) | 349.53 ± 25.25 | >500 |

*N*-butyl-1-deoxynojirimycin (**32**, Zavesca, Figure 9.4) is an approved drug for the treatment of Gaucher disease in a substrate reduction therapy.[17,18] This iminosugar is a potent ($IC_{50}$ = 50 μM[19]) reversible inhibitor of glucosylceramide synthase (GCS), which significantly relieved the symptoms of Gaucher patients. Later, the more hydrophobic analogue, AMP-DNM (**33**) was reported to be a 100-fold more potent GCS inhibitor ($IC_{50}$ = 0.2 μM[19]). Therefore, adamantane functionalized carba-cyclophellitol **34** (TB648) was designed as a potential GCS inhibitor.

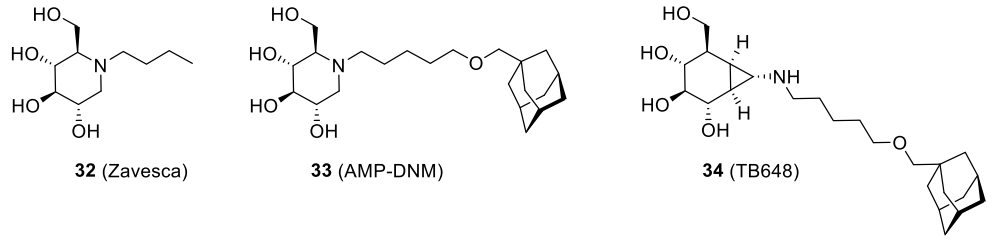


**Figure 9.4** The structures of potent (**32** and **33**) and potential (**34**) GCS inhibitors.

The synthesis of TB648 is described in Scheme 9.4. Treatment of compound **35** (**Chapter 6**) with diphenyl phosphoryl azide in the presence of triethylamine and *tert*-butanol resulted into compound **36**. Alkylation with 5-(adamant-1-yl-methoxy)-1-bromopentane[20], followed by global debenzylation and treatment with TFA gave target compound TB648 (**34**). The inhibition studies of TB648 towards GCS could not be performed in the timeframe of the here presented PhD research and will be performed in the near future.

Zavesca and AMP-DNM are potential β-glucosidase inhibitors.[20,21] The apparent $IC_{50}$ values were reassessed together with TB648 and extended to lysosomal α-glucosidase (GAA, Table 9.2). Zavesca and AMP-DNM inhibit GBA1 and GAA and more potently

**Scheme 9.4** The synthesis of TB648 (**34**).

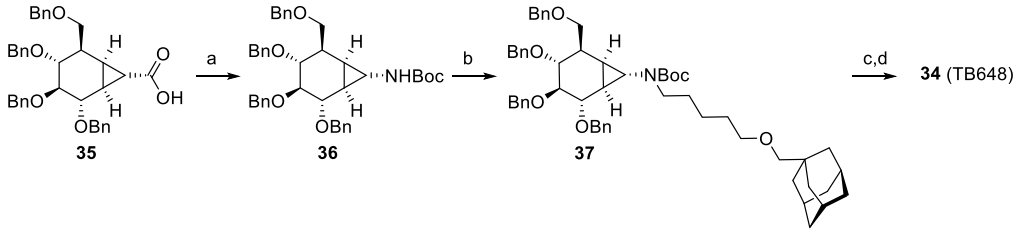


**Reagents and conditions**: a) $^t$BuOH, $Et_3N$, diphenyl phosphoryl azide, 90 °C, overnight, 51%; b) 5-(adamant-1-yl-methoxy)-1-bromopentane[20], NaH, DMF, rt, 3 h, 81%; c) 10% Pd/C, $H_2$, AcOH, MeOH, rt, 5 h; d) TFA, $CH_2Cl_2$, rt, 45 min, 80% over 2 steps.

GBA2. TB648 turned out to be selective for GBA1 with potency in the nanomolar range (Table 9.2). Selective inhibitors of lysosomal glucocerebrosidase (GBA1) are pursued as they may be exploited in pharmacological chaperone therapy for Gaucher disease. Herein, the folding of the enzyme in the endoplasmic reticulum may be stabilized to restore the GBA1 activity.[21] TB648 may therefore be exploited as a selective modulator of GBA1 in a clinical setting.

**Table 9.2** The apparent $IC_{50}$ values of Zavesca (**32**), AMP-DNM (**33**) and TB648 (**34**) towards GBA1, GBA2 and GAA in μM.

| Compound | Human β-glucosidases | | Human α-glucosidase |
|---|---|---|---|
| | GBA1 | GBA2 | GAA |
| Zavesca (**32**) | 604.40 ± 12.59 | 0.14 ± 0.01 | 39.37 ± 2.45 |
| AMP-DNM **(33)** | 0.178 ± 0.003 | 0.0007 ± 0.0003 | 2.96 ± 0.07 |
| TB648 (**34**) | 0.0111 ± 0.0008 | 47.91 ± 2.72 | >1000 |

The $B_{2,5}$ transition-state is expected for mannosidases, unlike β-glucosidases or α-galactosidases. This may explain the lower potency of mannopyranose-configured cyclophellitols towards mannosidases (**Chapter 4** and **Chapter 5**) and therefore $B_{2,5}$ conformed compounds are interesting targets. The conformation of the bicyclic aziridine **38** was determined by *J*-coupling constant analysis and turned out to be predominantly $B_{1,4}$ (Figure 9.5).[22] This conformation resembles the conformation of oxocarbenium ion transition-state (**39**) present in the itinerary of α-mannosidases. This led to the design of bicyclic cyclopropyl **40** which may adopt a boat conformation as well. By altering of the hydroxyl conformations, a close mimic of **39** could be obtained and as such be a potential reversible α-mannosidases inhibitor.

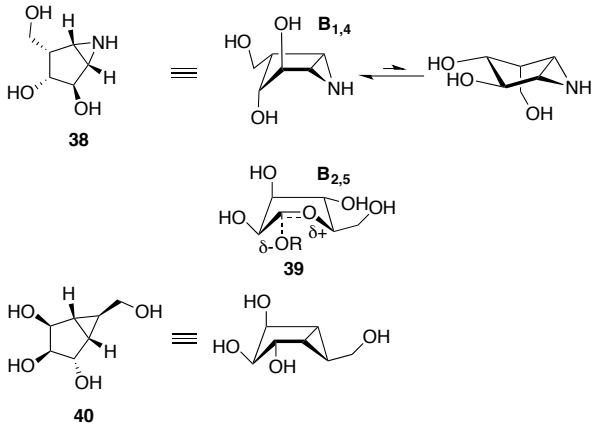


**Figure 9.5** Bicyclic aziridine **38** adopts predominantly the $B_{1,4}$ conformation[22] and therefore bicyclic cyclopropyl **40** is proposed to be a conformational mimic of the oxocarbenium ion transition-state of α-mannosidases.

The putative synthesis of bicyclic cyclopropyl **40** is depicted in Scheme 9.5. Cyclopentene **41**[23] could be treated with HCl in a mixture of THF and $H_2O$ and subsequently benzylated to obtain compound **42**. Cyclopropanation with EDA as described in **Chapter 6** may give compound **43**. Reduction of the ester followed by palladium-catalyzed hydrogenation may give target compound **40**.

**Scheme 9.5** The putative synthesis of bicyclic cyclopropyl **40**.

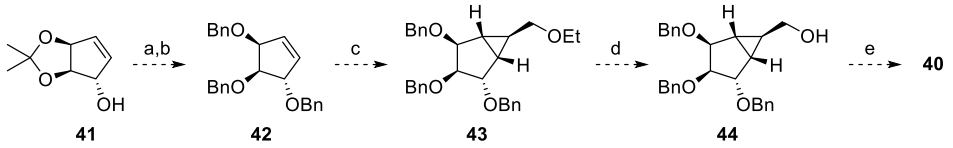


**Reagents and conditions:** a) HCl, THF, MeOH; b) BnBr, NaH, DMF; c) EDA, $Cu(acac)_2$, EtOAc; d) DIBAL, THF; e) $Pd(OH)_2/C$, $H_2$, MeOH.

The substrate specificity of β-mannosidase over α-mannosidases is determined in part by the conformation of the aglycon. Bicyclic cyclopropyl **46** with the 2-hydroxyl group in axial position may result in a selective β-mannosidases inhibitor (Figure 9.6). The synthesis of this conformational analogue can be commenced with cyclopentene **47**.[24] Global benzylation of compound **47**, followed by cyclopropanation with EDA may give bicyclic cyclopropyl **49**. After DIBAL-mediated reduction of **49** and palladium-catalyzed hydrogenolysis target compound **46** could be obtained.

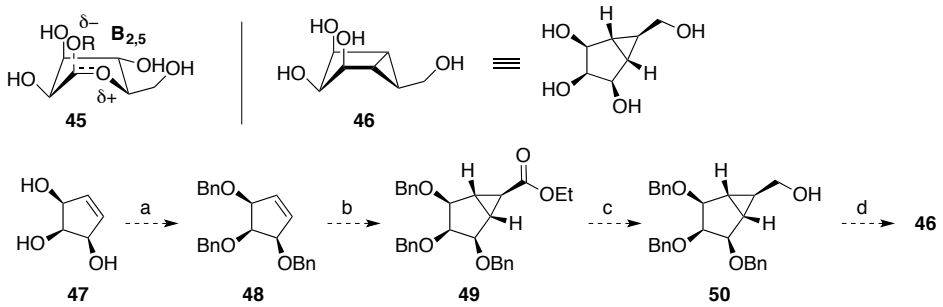


**Figure 9.6** Bicyclic cyclopropyl **46** is proposed to be a conformational mimic of the oxocarbenium ion transition-state of β-mannosidases (**45**). Reagents and conditions: a) BnBr, NaH, DMF; b) EDA, $Cu(acac)_2$, EtOAc; c) DIBAL, THF; d) $Pd(OH)_2/C$, $H_2$, MeOH.

The glycan metabolism is controlled by glycosidases together with glycosyltransferases (GTs). Potent GTs inhibitors, however, are scarce and often sought after as potential GT regulators. Based on the results of carba-cyclophellitols as analogues of the oxocarbenium ion-like transition-state, the synthesis of two potential carba-cyclophellitol based galactosyltransferase (GalT) inhibitors (**51** and **52**, Figure 9.7) is described in **Chapter 8**. A *O*-sulfamoyl- (**51)** or a phosphate moiety (**52**) was introduced to mimic the substrate and enhance the potency towards GalTs.

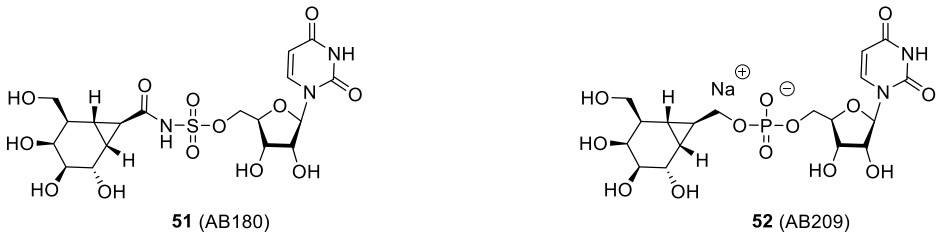


**Figure 9.7** Potential carba-cyclophellitol based galactosyltransferase (GalT) inhibitors.

Carba-cylophellitol UDP **57** may be an attractive target that could be obtained following the same synthetic strategy (Scheme 9.6A). After obtaining monophosphate **55**, the benzyl ethers may be removed with palladium-catalyzed hydrogenation. Coupling of phosphate **56** with phosphoramidite **58** using the previously described methodology could result into carba-cylophellitol UDP **57**. As described by Wagner and co-workers, introduction of a formylthienyl moiety at position 5 of the uracil base of Gal-UDP resulted in an up to 10-fold lower $K_i$ compared to the $K_m$ of the natural donor towards various galactosyltransferases.[25] Therefore, Gal-UPD derivative **62** may be a more potent inhibitor towards galactosyltransferases (Scheme 9.6B). The proposed

synthetic route towards compound **62** starts with 5-iodouridine-5'-phosphoromorpholidate **60** which can be obtained from uridine (**59**) in 48% over three steps.[25] Subsequently, tetrazole catalyzed coupling with carba-cyclophellitol **56**, Suzuki coupling with (5-formyl-2-thienyl)boronic acid, deacetylation and treatment with Dionex sodium exchange resin may result in 5-(5-formylthien-2-yl) UDP carba-cyclophellitol **62** as a sodium salt.

**Scheme 9.6** The putative synthesis compound **57** and compound **62**.

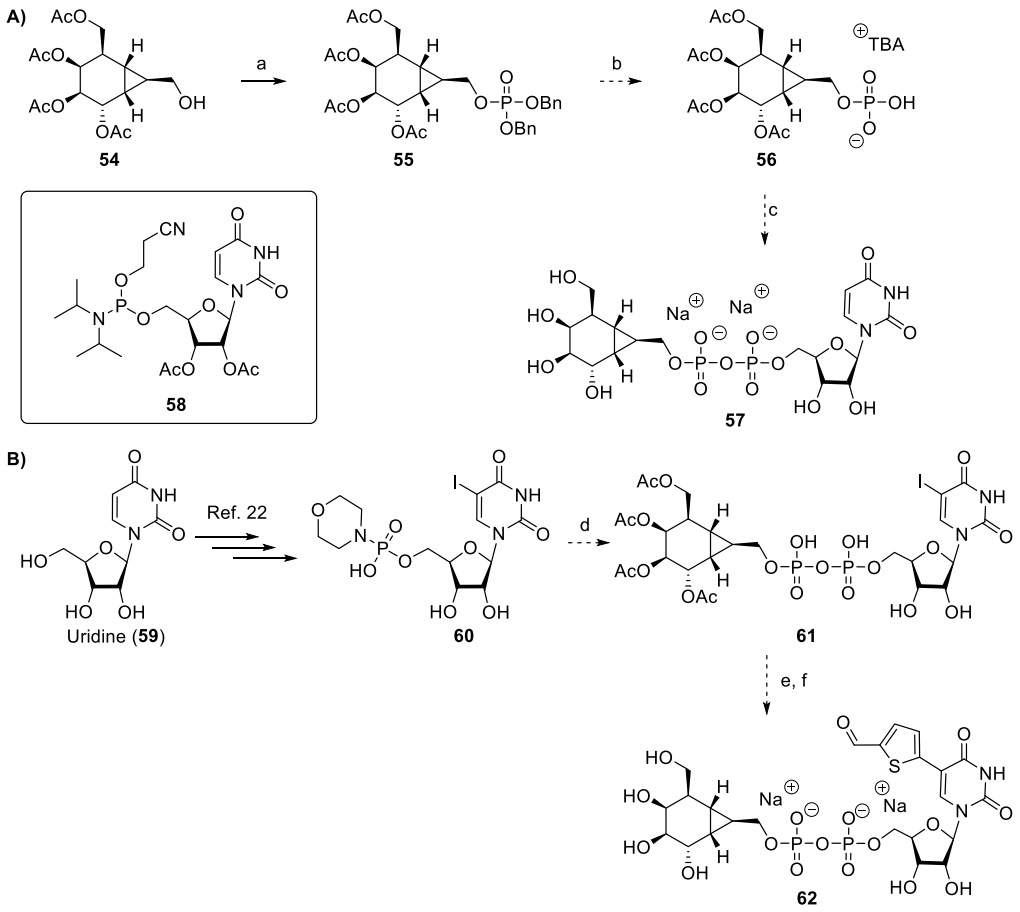


**Reagents and conditions:** a) tetrabenzyl pyrophosphate, LDA, THF, - 78 °C to rt, 2 h, 17%; b) *i*) $H_2$, Pd/C 10%, MeOH, rt; *ii*) tertbutylammonium hydroxide (TBA-OH) 40% aqueous solution, lyophilisation; c) *i*) **58**[26], DCI, MeCN, rt; *ii*) $^t$BuOOH, rt; *ii*) DBU, rt,; *iii)* $Et_3N/H_2O$/MeOH (1:1:3), rt; *iv*) size-exclusion, HPLC purification, Dionex sodium exchange; d) **56**, tetrazole, DMF, rt; e) (5-formyl-2-thienyl)boronic acid, $Na_2Cl_4Pd$, trisodium salt of triphenylphosphine-3,3',3''-trisulfonic acid

(TPPTS), $Cs_2CO_3$, $H_2O$, 50 °C; f) $Et_3N/H_2O/MeOH$ (1:3:1), rt, size-exclusion, HPLC purification, Dionex sodium exchange.

To determine the potency of GalT inhibitors, the donor and acceptor substrate are required. The donor substrate of GTB, for example, is commercially available (UDP-α-D-galactose as a disodium salt). A simplified acceptor substrate, α-L-Fuc*p*-(1→2)-β-D-Gal*p*-O-$(CH_2)_8N_3$ **63** (Figure 9.8), can be synthesized (see experimental). Although this is a simplified structure of the acceptor, similar structures were tolerated by GTB.[27,28]

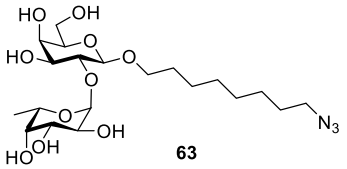


**Figure 9.8** Structure of acceptor substrate **63**.

After having the donor and acceptor analogue **63** in hand a spectroscopic assay with a cascade of reactions, such as the commercial available Malachite green assay, can be performed to determine the inhibition potency of a potential inhibitor by a fluorescent output (Figure 9.9). In this assay, phosphatases will give inorganic phosphate ($P_i$) from the GTB produced UDP. After formation of $P_i$, a solution of ammonium molybdate in diluted sulfuric acid will be added followed by the addition of malachite green oxalate. Finally, the absorbance at 620 nm of the obtained malachite phosphomolybdate complex is proportional with the conversion of GTB.

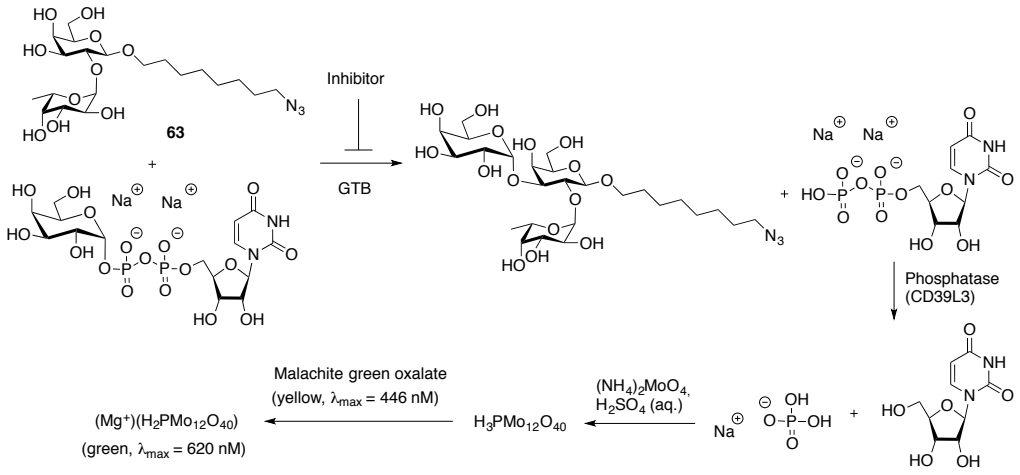


**Figure 9.9** GTB based biochemical activity assay.

Additionally compound **51** (AB180) and **52** (AB209) were examined towards galactosidases. AB180 turned out to be the first potent carba-cyclophellitol based α-GalA inhibitor (Table 9.3).

**Table 9.3** The apparent $IC_{50}$ values of **51** and **52** towards GALC and α-GalA in μM.

| Compound | β-galactosidase (GALC) | α-galactosidase (α-GalA) |
|---|---|---|
| **51** (AB180) | 180.27 ± 4.52 | 18.84 ± 1.33 |
| **52** (AB209) | >500 | >500 |

In the second part of **Chapter 8**, compound ML128 (**64**) was synthesized and analysed towards glucosylceramide synthase (GCS) as well as towards α-glucosidases (GAA and GANAB) and β-glucosidases (GBA1 and GBA2). However, no inhibition was observed. ML131 (**65**), an analogue of **64**, was synthesized in a similar manner (Figure 9.10).

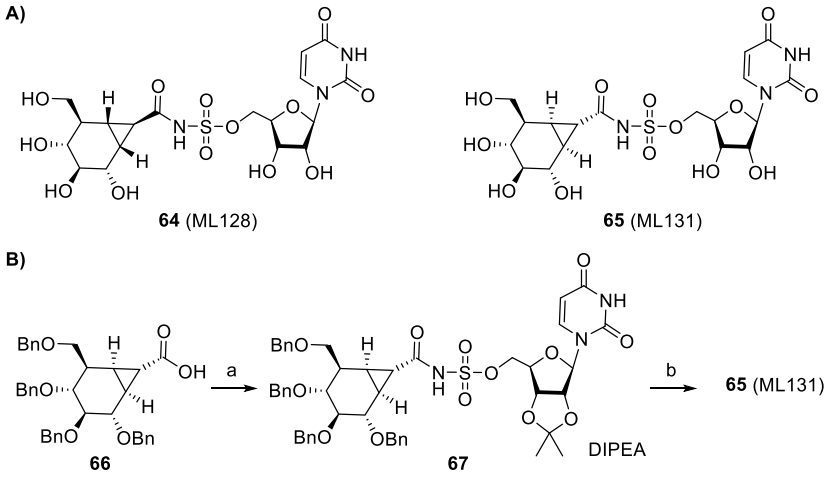


**Figure 9.10** A) Structures of compound **64** (ML128) and **65** (ML131). B) Synthesis of β-glucopyranose-configurated carba-cyclophellitol **65** (ML131). Reagents and conditions: a) *i*) oxalyl chloride, toluene, 40 °C, 5 h; *ii*) 2',3'-O-isopropylidene-5'-O-sulfamoyluridine, N,N-diisopropylethylamine, $CH_2Cl_2$, rt, overnight, size-exclusion, 86%; b) *i*) $BCl_3$, $CH_2Cl_2$, 0 °C, 3 h; *ii*) MeOH, HPLC purification, 20%.

The inhibitory potency of ML131 **65** was determined towards GBA1, GBA2, GAA and GANAB (all glycosidases) and GCS (a glycosyl transferase) in a similar fashion as for compound **64**. ML131 turned out to be micromolar active towards GBA1 and GBA2

(Table 9.4), similar to the most potent carba-cyclophellitol analogue reported in **Chapter 7**, DW082.

**Table 9.4** Apparent $IC_{50}$ values of compound **65** towards glucosyltranferase and glycosidases (μM).

| Compound | β-glucosidase | | α-glucosidase | | GlucT |
|---|---|---|---|---|---|
| | GBA1 | GBA2 | GAA | GANAB | GCS |
| **65** (ML131) | 26.18 ± 0.75 | 138.90 ± 8.48 | >100 | >100 | >50 |

## Experimental

**General methods:** All chemicals were purchased from Acros, Sigma Aldrich, Biosolve, VWR, Fluka, Merck and Fisher Scientific and used as received unless stated otherwise. Dichloromethane (DCM), tetrahydrofuran (THF), *N*,*N*-dimethylformamide (DMF) and toluene were stored over flame-dried 4 Å molecular sieves before use. Pyridine was stored on KOH pellets before use. Traces of water from reagents were removed by co-evaporation with toluene in reactions that require anhydrous conditions. All reactions were performed under an argon atmosphere unless stated otherwise. TLC analysis was conducted using Merck aluminium sheets (Silica gel 60 $F_{254}$) with detection by UV absorption (254 nm), by spraying with a solution of $(NH_4)_6Mo_7O_{24}{\cdot}4H_2O$ (25 g/L) and $(NH_4)_4Ce(SO_4)_4{\cdot}2H_2O$ (10 g/L) in 10% sulfuric acid, a solution of $KMnO_4$ (20 g/L) and $K2CO_3$ (10 g/L) in water or ninhydrin (0.75 g/L), followed by charring at ~150 ˚C. Column chromatography was performed using Screening Device b.v. Silica Gel (particle size of 40 – 63 μm, pore diameter of 60 Å) in the indicated solvents. For reversed-phase HPLC purifications an Agilent Technologies 1200 series instrument equipped with a semiprep column (Gemini C18, 250 x 10 mm, 5 μm particle size, Phenomenex) was used. LC/MS analysis was performed on a Surveyor HPLC system (Thermo Finnigan) equipped with a $C_{18}$ column (Gemini, 4.6 mm x 50 mm, 5 μm particle size, Phenomenex), coupled to a LCQ Adventage Max (Thermo Finnigan) ion-trap spectrometer ($ESI^+$). The applied buffers were $H_2O$ (A) and MeCN with 1% aqueous TFA (B). Optical rotations were measured on a Propol automatic polarimeter. $^{31}P$ NMR, $^{1}H$ NMR and $^{13}C$ NMR spectra were recorded on a Brüker AV-400 (161.7, 400 and 101 MHz respectively) spectrometer in the given solvent. Chemical shifts are given in ppm (δ) relative to the residual solvent peak or tetramethylsilane (0 ppm) as internal standard. Coupling constants are given in Hz. High-resolution mass spectrometry (HRMS) analysis was performed with a LTQ Orbitrap mass spectrometer (Thermo Finnigan), equipped with an electronspray ion source in positive mode (source voltage 3.5 kV, sheath gas flow 10 mL/min, capillary temperature 250 °C) with resolution R = 60000 at m/z 400 (mass range m/z = 150 – 2000) and dioctyl phthalate (m/z = 391.28428) as a "lock mass". The high-resolution mass spectrometer was calibrated prior to measurements with a calibration mixture (Thermo Finnigan).

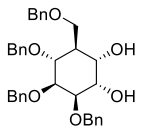

**(1*S*,2*S*,3*R*,4*S*,5*R*,6*S*)-3,4,5-tris(benzyloxy)-6-((benzyloxy)methyl)cyclohexane-1,2-diol (4)**

To a solution of cyclohexene **3** (1.04 g, 2.0 mmol) in EtOAc/ACN (1:1, 60 mL) was added a solution of sodium periodate (0.641 g, 3 mmol, 1.5 eq.) and catalytic amount of ruthenium(III) chloride trihydrate (36 mg, 0.14 mmol, 0.07 eq.) in $H_2O$ (16 mL) at 0 °C. After vigorously stirring for 1 h, the reaction mixture was quenched with 10% aqueous $Na_2S_2O_3$ (15 mL) and diluted with saturated aqueous $NaHCO_3$ and EtOAc. The aqueous layer was separated and extracted with EtOAc (3 x). The combined organic layers were washed with brine, dried over $MgSO_4$ and concentrated *in vacuo*. Purification by column chromatography (30% EtOAc in pentane → 40% EtOAc in pentane) gave diol **4** (0.746 g, 1.34 mmol, 68%) as a clear oil. $^1$H NMR (400 MHz, $CDCl_3$) δ 7.40 – 7.24 (m, 18H), 7.22 – 7.17 (m, 2H), 4.89 (d, *J* = 11.0 Hz, 1H), 4.78 (d, *J* = 12.2 Hz, 1H), 4.69 – 4.59 (m, 3H), 4.49 (s, 2H), 4.45 (d, *J* = 10.9 Hz, 1H), 4.06 – 3.91 (m, 5H), 3.64 (t, *J* = 9.3 Hz, 1H), 3.56 (t, *J* = 9.0 Hz, 1H), 2.60 (s, 1H), 2.23 (qd, *J* = 9.4, 3.3 Hz, 1H). $^{13}$C NMR (101 MHz, $CDCl_3$) δ 138.7, 138.5, 138.5, 137.4, 128.6, 128.4, 128.1, 128.0, 127.8, 127.7, 127.6, 81.2, 75.9, 75.7, 75.0, 73.6, 73.3, 72.6, 71.9, 71.8, 71.8, 70.0, 42.7. HRMS: calculated for $[C_{35}H_{38}O_6]^+$ 555.27412, found 555.27433.

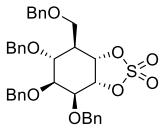

**(3a*R*,4*S*,5*S*,6*R*,7*R*,7a*S*)-4,5,6-tris(benzyloxy)-7-((benzyloxy)methyl)hexahydrobenzo[d][1,3,2]dioxathiole 2,2-dioxide (5)**

Diol **4** (0.36 g, 0.65 mmol) was dissolved in $CH_2Cl_2$ (30 mL) and $Et_3N$ (0.33 mL, 2.4 mmol, 3.7 eq.) was added at 0 °C. Next, thionyl chloride (0.15 mL, 2.1 mmol, 3.2 eq.) was slowly added over 5 min. After stirring for 1 h, additional $Et_3N$ (90 µL, 0.65 mmol, 1 eq.) and thionyl chloride (45 µL, 0.65 mmol, 1 eq.) was added. The reaction mixture was stirred for an additional 30 min before quenching with cold $H_2O$ and dilution with cold $Et_2O$. The layers were separated and the organic layer was washed with $H_2O$ (2 x), dried over $MgSO_4$, filtered and concentrated *in vacuo*. Purification by column chromatography (3.5% EtOAc in pentane) gave the sulphite diastereomeric mixture (390 mg) as an orange oil. HRMS: calculated for $[C_{35}H_{37}O_7S]^+$ 601.22545, found 601.22584. To a solution of the sulphite diastereomeric mixture (192 mg, 0.32 mmol) in $CCl_4$/MeCN (1:1, 24 mL) was added a solution of sodium periodate (0.137 g, 0.64 mmol, 2.0 eq.) and a catalytic amount of ruthenium(III) chloride trihydrate (6 mg, 22 µmol, 0.07 eq.) in $H_2O$ (12 mL) at 0 °C. After vigorously stirring for 1.5 h, the reaction mixture was diluted with $Et_2O$ and $H_2O$. The organic layer was separated, washed with brine, dried over $MgSO_4$ and concentrated *in vacuo*. Purification by column chromatography (8% EtOAc in pentane) gave title compound (81 mg, 0.131 mmol, 41% over 2 steps) as a white solid. $^1$H NMR (400 MHz, $CDCl_3$) δ 7.40 – 7.20 (m, 18H), 7.14 (dd, *J* = 7.3, 2.2 Hz, 2H), 5.29 (dd, *J* = 11.2, 6.4 Hz, 1H), 5.20 (t, *J* = 6.2 Hz, 1H), 4.73 (dd, *J* = 19.8, 11.8 Hz, 1H), 4.59 (d, *J* = 4.2 Hz, 2H), 4.59 – 4.51 (m, 1H), 4.43 (d, *J* = 11.7 Hz, 2H), 4.31 (d, *J* = 11.9 Hz, 1H), 4.22 (d, *J* = 11.5 Hz, 1H), 4.11 (d, *J* = 1.6 Hz, 1H), 3.82 – 3.77 (m, 2H), 3.62 – 3.46 (m, 2H), 2.26 – 2.16 (m, 1H). $^{13}$C NMR (101 MHz, $CDCl_3$) δ 138.0, 137.6, 137.5, 137.4, 128.7, 128.6, 128.5, 128.2, 128.1, 128.0, 127.9, 127.7, 83.6, 80.0, 76.5, 74.2, 73.2, 72.9, 72.8, 72.6, 64.8, 42.5. HRMS: calculated for $[C_{35}H_{36}O_8SNa]^+$ 639.20231, found 639.20238.

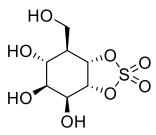

**(3a*R*,4*S*,5*S*,6*R*,7*R*,7a*S*)-4,5,6-trihydroxy-7-(hydroxymethyl)hexahydrobenzo[d][1,3,2]dioxathiole 2,2-dioxide (6, TB612)**

Benzylated sulphate **5** (70 mg, 0.11 mmol) was dissolved in MeOH (10 mL). The reaction mixture was purged with nitrogen gas and 10% palladium on carbon (15 mg) was added. After the reaction vessel was purged with hydrogen gas and vigorously stirring overnight, the palladium catalyst was filtered off followed by concentration *in vacuo*. Purification by column chromatography (10% MeOH in DCM → 20% MeOH in DCM) resulted compound **6** (14 mg, 55 µmol, 50%) as a clear oil. $^{1}$H NMR (500 MHz, MeOD) δ 4.20 (d, *J* = 2.0 Hz, 1H), 4.15 (d, *J* = 5.2 Hz, 1H), 4.08 (d, *J* = 5.3 Hz, 1H), 4.04 – 3.97 (m, 1H), 3.79 – 3.73 (m, 1H), 3.59 (dd, *J* = 10.6, 6.3 Hz, 1H), 3.51 – 3.43 (m, 1H), 2.25 – 2.20 (m, 1H). $^{13}$C NMR (126 MHz, MeOD) δ 88.3, 83.2, 82.6, 76.2, 74.3, 64.1, 45.7.

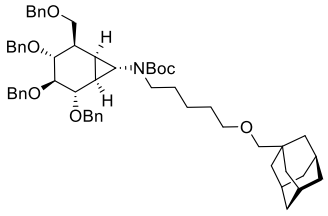

***tert*-butyl (5-(((3*R*,5*R*)-adamantan-1-yl)methoxy)pentyl)((1*S*,2*S*,3*R*,4*R*,5*R*,6*S*,7*S*)-2,3,4-tris(benzyloxy)-5-((benzyloxy)methyl)bicyclo[4.1.0]heptan-7-yl)carbamate (37)**

To a solution of carboxylic acid **35** (80 mg, 0.138 mmol) in *tert*-butanol (4 mL) was added triethylamine (21 µL, 0.152 mmol, 1.1 eq.) and diphenylphosphorylazide (33 µL, 0.152 mmol, 1.1 eq.). The reaction mixture was heated to 90 °C and stirred overnight. The solution was concentrated *in vacuo*, redissolved in EtOAc (15 mL) and washed with HCl (1 M) and saturated aqueous $NaHCO_3$. The organic layer was dried over $MgSO_4$ and concentrated *in vacuo*. Purification by column chromatography (10% EtOAc in pentane → 20% EtOAC in pentane) gave compound **36** (45 mg, 0.069 mmol, 51%) as a white solid. HRMS: calculated for $[C_{41}H_{48}NO_6]^+$ 650.34761, found 650.34826. Compound **36** (9.1 mg, 14.1 µmol) was taken up in DMF (0.14 mL) and subsequently 5-(adamant-1-yl-methoxy)-1-bromopentane (18 mg, 56 µmol, 4 eq.) and NaH (60% dispersion in mineral oil, 4.0 mg, 0.10 mmol, 7 eq.) were added at room temeprature. After stirring for 3 h, the reaction mixture was diluted with $Et_2O$ and washed with aqueous HCl (0.1 M). The water layer was extracted with $Et_2O$ (3 x) and the combined organic layers were dried over $MgSO_4$ and concentrated *in vacuo*. Purification by column chromatography (4% EtOAc in pentane → 8% EtOAc in pentane) gave title compound **37** (10.1 mg, 11.4 µmol, 81%) as a clear oil. $^{1}$H NMR (400 MHz, $CDCl_3$) δ 7.40 (d, *J* = 7.1 Hz, 2H), 7.37 – 7.20 (m, 16H), 7.13 (dd, *J* = 6.7, 2.9 Hz, 2H), 4.88 (d, *J* = 11.0 Hz, 2H), 4.82 – 4.73 (m, 3H), 4.49 (d, *J* = 2.5 Hz, 2H), 4.36 (d, *J* = 10.8 Hz, 1H), 3.88 (d, *J* = 8.0 Hz, 1H), 3.78 (dd, *J* = 8.7, 2.9 Hz, 1H), 3.66 (t, *J* = 6.7 Hz, 1H), 3.54 (d, *J* = 7.8 Hz, 1H), 3.50 (d, *J* = 8.5 Hz, 1H), 3.30 (t, *J* = 6.5 Hz, 2H), 3.04 – 2.98 (m, 1H), 2.93 (d, *J* = 2.5 Hz, 2H), 2.42 – 2.35 (m, *2*H), 1.94 (s, 3H), 1.75 – 1.16 (m, 22H). HRMS: calculated for $[C_{57}H_{74}NO_7]^+$ 884.54598, found 884.54680.

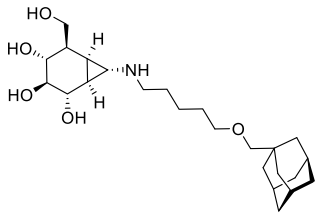

**(1*S*,2*S*,3*R*,4*R*,5*R*,6*S*,7*S*)-7-((5-(((3*R*,5*R*)-adamantan-1-yl)methoxy)pentyl)amino)-5-(hydroxymethyl)bicyclo[4.1.0]heptane-2,3,4-triol (34, TB648)**

Compound **37** (9.5 mg, 10 µmol) was dissolved in MeOH (1 mL). A few drops of acetic acid (glacial) and 10% Pd on carbon (8 mg) were added and the reaction vessel was purged with hydrogen gas. After vigorously stirring for 5 h at room temperature, the solution was filtered and concentrated *in vacuo*. The residue was dissolved in $CH_2Cl_2$/trifluoroacetic acid (1.6 mL, 1:1) and stirred for 45 min at room temperature. The reaction mixture was concentrated *in vacuo* an purification by HPLC purification (C18, linear gradient: 30-36% B in A, solutions used A: $H_2O$, B: acetonitrile, 0.5% TFA) yielded adamantane **34** (3.4 mg, 8.1 µmol, 80%) as a clear oil. LC/MS analysis: $R_t$ 5.6 min (linear gradient 10% → 90% B in 12.5 min, ). $^1$H NMR (850 MHz, MeOD) δ 4.62 (s, 1H), 3.93 (dd, *J* = 10.5, 4.5 Hz, 1H), 3.61 (dd, *J* = 10.5, 7.9 Hz, 1H), 3.47 (dd, *J* = 8.4, 1.2 Hz, 1H), 3.39 (t, *J* = 6.4 Hz, 2H), 3.09 (dd, *J* = 10.0, 8.5 Hz, 1H), 2.97 (s, 2H), 2.80 (t, *J* = 10.2 Hz, 1H), 2.69 (t, *J* = 7.6 Hz, 2H), 2.03 – 1.98 (m, 1H), 1.94 (s, *J* = 7.9 Hz, 1H), 1.91 (d, *J* = 7.5 Hz, 1H), 1.77 (s, 1H), 1.75 (s, 1H), 1.69 (s, 1H), 1.68 (s, 1H), 1.61 – 1.57 (m, 2H), 1.56 (s, 2H), 1.56 (s, 2H), 1.55 – 1.51 (m, 2H), 1.44 – 1.38 (m, 2H), 1.37 – 1.30 (m, 2H), 1.22 (s, 2H), 1.06 (dd, *J* = 9.6, 1.0 Hz, 1H). $^{13}$C NMR (214 MHz, MeOD) δ 83.1, 79.4, 74.6, 72.5, 71.0, 64.9, 50.1, 49.3, 49.2, 49.1, 49.0, 48.9, 48.8, 48.7, 43.6, 40.8, 39.7, 38.3, 31.1, 30.6, 30.2, 29.8, 26.2, 25.1, 23.8. HRMS: calculated for $[C_{24}H_{42}NO_5]^+$ 424.30575, found 424.30580

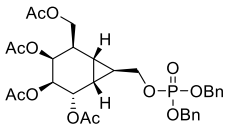

**(1*R*,2*S*,3*R*,4*S*,5*R*,6*R*,7*R*)-5-(acetoxymethyl)-7-(((bis(benzyloxy)phosphoryl)oxy)methyl)bicycle[4.1.0]heptane-2,3,4-triyl triacetate (55)**

Alcohol **54** (142 mg, 0.38 mmol) was dissolved in THF (5 mL), cooled to -78 °C and lithium diisopropylamide (2 M in THF, 0.21 mL, 0.42 mmol, 1.1 eq.) was added. After stirring for 5 min, tetrabenzyl pyrophosphate (0.246 g, 0.46 mmol, 1.2 eq.) in THF (2 mL) was added. The reaction mixture was stirred for 3 h, before being quenched with saturated aqueous $NaHCO_3$, extracted with EtOAc and washed with brine. The aqueous layer was extracted once with EtOAc. The combined organic layers were dried over $MgSO_4$, filtered and concentrated *in vacuo*. Purification by column chromatography (20% EtOAc in pentane → 50% EtOAc in pentane) gave compound **55** (42 mg, 66 µmol, 17%) as a white solid. $^{31}$P NMR (162 MHz, $CDCl_3$): δ = -0.47. $^1$H NMR (400 MHz, $CDCl_3$): δ 7.37 (s, 10H), 5.36 (dd, *J* = 9.2, 6.8 Hz, 1H), 5.26 (s, 1H), 5.08 – 4.98 (m, 4H), 4.55 (dd, *J* = 9.3, 1.6 Hz, 1H), 4.10 – 3.94 (m, 2H), 3.85 – 3.67 (m, 2H), 2.16 – 2.13 (m, 1H), 2.10 – 2.00 (m, 12H), 1.67 – 1.63 (m, 1H), 1.11 – 1.03 (m, 1H), 0.80 – 0.71 (m, 1H). $^{13}$C NMR (100 MHz, $CDCl_3$): δ 171.0, 170.8, 170.6, 170.3, 135.9, 135.8, 128.8, 128.1, 72.1, 70.2, 70.2, 69.5, 69.4, 69.4, 69.2, 69.0, 62.8, 38.0, 24.4, 24.3, 21.3, 21.2, 20.9, 20.9 20.8, 18.5. HRMS: Calculated for $[C_{31}H_{38}O_{12}P]^+$ 633.20954, found 633.21000.

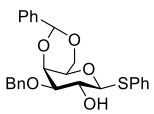

**Phenyl 3-*O*-benzyl-4,6-*O*-benzylidene-1-thio-β-D-galactopyranoside (68)**

To a solution of phenyl 4,6-*O*-benzylidene-1-thio-β-D-galactopyranoside[29] (6.49 g, 18.0 mmol) in toluene (45 mL) was added dibutyltinoxide (4.52 g, 18.2 mmol).[30] After reflux overnight in a Dean-Stark apparatus the reaction mixture was

concentrated *in vacuo*. The resulting mixture was redissolved in DMF (45 mL) and CsF (5.46 g, 36.0 mmol) and BnBr (3.21 mL, 27.0 mmol) were added. After stirring for 3 h at room temperature the reaction mixture was quenched with MeOH, filterated over celite and concentrated *in vacuo*. Purification by silica chromatography (5% EtOAc in toluene → 6% EtOAc in toluene) resulted in compound **68** (5.18 g, 11.5 mmol, 64%) as a white solid. $[\alpha]D^{20}$ = -8.0 (*c* = 0.1, $CHCl_3$). $^1$H NMR (400 MHz, $CDCl_3$): δ = 7.71 – 7.64 (m, 2H), 7.47 – 7.11 (m, 13), 5.41 (s, 1H), 4.71 (d, *J* = 4.0 Hz, 2H), 4.50 (d, *J* = 9.5 Hz, 1H), 4.34 (dd, *J* = 12.3, 1.3 Hz, 1H), 4.12 (d, *J* = 3.2 Hz, 1H), 4.00 – 3.89 (m, 2H), 3.49 (dd, *J* = 9.3, 3.3 Hz, 1H), 3.41 (s, 1H), 2.47 (s, 1H). $^{13}$C NMR (101 MHz, CDCl3): δ = 138.0, 137.9, 133.8, 130.7, 129.1, 129.0, 128.6, 128.2, 128.2, 128.0, 126.6, 101.2, 87.1, 80.3, 73.3, 71.7, 70.1, 69.5, 67.2. HRMS: calculated for $[C_{26}H_{27}O_5S]^+$ 451.15737; found 451.15749.

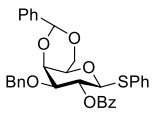


**Phenyl 2-*O*-benzoyl-3-*O*-benzyl-4,6-*O*-benzylidene-1-thio-β-D-galactopyranoside (69)**

To a solution alcohol **68** (90 mg, 0.2 mmol) in pyridine (0.5 mL) was added benzoyl chloride (26 µL, 0.22 mmol). After stirring overnight at room temperature the reaction mixture was diluted with EtOAc, washed with $H_2O$ and brine. The organic layer was dried with $MgSO_4$, filtered and concentrated *in vacuo*. Purification by silica chromatography (5% EtOAc in toluene) yielded in compound **69** (110 mg, 0.2 mmol, quant.) as a white solid. $[\alpha]D^{20}$ = -6.0 (*c* = 1.0, $CHCl_3$). $^1$H NMR (400 MHz, $CDCl_3$): δ = 8.12 (d, *J* = 7.6 Hz, 2H), 8.04 (d, *J* = 7.9 Hz, 2H), 7.59 – 7.09 (m, 16H), 5.57 (t, *J* = 9.7 Hz, 1H), 5.48 (s, 1H), 4.80 (d, *J* = 9.8 Hz, 1H), 4.67 – 4.51 (m, 2H), 4.37 (d, *J* = 12.2 Hz, 1H), 4.24 (d, *J* = 3.1 Hz, 1H), 4.01 (d, *J* = 12.2 Hz, 1H), 3.76 (dd, *J* = 9.6, 3.2 Hz, 1H), 3.48 (s, 1H). $^{13}$C NMR (101 MHz, $CDCl_3$): δ = 172.1, 165.1, 137.7, 133.90, 133.8, 133.1, 131.7, 130.3, 130.3, 130.0, 129.1, 128.8, 128.6, 128.5, 128.4, 128.2, 128.1, 127.8, 127.8, 126.7, 101.4, 85.5, 78.2, 73.2, 71.1, 70.2, 69.4, 69.1. HRMS: calculated for $[C_{33}H_{31}O_6S]^+$ 555.18359; found 555.18380.

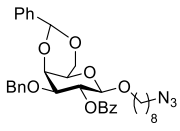


**8-azidooctane 2-*O*-benzoyl-3-*O*-benzyl-4,6-*O*-benzylidene-β-D-galactopyranoside (70)**

Compound **69** (124mg, 0.73 mmol) and 8-azidooctan-1-ol[31] (443 mg, 0.8 mmol) were dissolved in $CH_2Cl_2$ (4 mL), after which activated molecular sieves (4 Å) were added. The reaction mixture was cooled to -45 °C and subsequently *N*-iodosuccinimide (392 mg, 1.74 mmol) and TMSOTf (33 µL, 184 µmol) were added. After stirring for 30 min at -40 °C the reaction mixture was quenched at 0 °C with $Et_3N$ (1 mL), diluted with $CHCl_3$ and washed with $Na_sS_2O_3$ and $H_2O$. The organic layer was dried with $MgSO_4$, filtered and concentrated *in vacuo*. Purification by column chromatography (30% EtOAc in pentane → 50% EtOAc in pentane) gave compound **70** (380 mg, 618 µmol, 85%) as a clear yellow oil. $^1$H NMR (400 MHz, $CDCl_3$): δ = 8.04 (d, *J* = 7.1 Hz, 2H), 7.63 – 7.54 (m, 4H), 7.45 (t, *J* = 7.7 Hz, 2H), 7.40 – 7.32 (m, 3H), 7.28 – 7.14 (m, 4H), 5.63 (dd, *J* = 10.0, 8.0 Hz, 1H), 5.52 (s, 1H), 4.69 (d, *J* = 12.9 Hz, 1H), 4.60 (d, *J* = 12.9 Hz, 1H), 4.54 (d, *J* = 8.0 Hz, 1H), 4.37 – 4.29 (m, 1H), 4.24 (d, *J* = 3.4 Hz, 1H), 4.07 (dd, *J* = 12.3, 1.5 Hz, 1H), 3.94 – 3.87 (m, 1H), 3.74 (dd, *J* = 10.1, 3.5 Hz, 1H), 3.48 – 3.37 (m, 2H), 3.16 (t, *J* = 7.0 Hz, 2H), 1.47 – 1.39 (m, 3H), 1.21 – 1.00 (m, 9H). $^{13}$C NMR (101 MHz, $CDCl_3$): δ = 165.2, 138.0, 137.8, 133.0, 130.4, 129.9, 129.0, 128.4, 128.4, 128.2, 127.8, 126.6, 101.4, 101.3, 77.0, 73.2, 70.9, 70.9, 69.3, 69.3, 66.7, 51.5, 29.4, 29.1, 29.0, 28.8, 26.6, 25.8. HRMS: calculated for $[C_{35}H_{42}N_3O_7]^+$ 616.30173; found 616.30190

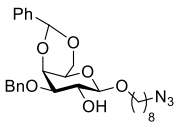

**8-azidooctane 3-*O*-benzyl-4,6-*O*-benzylidene-β-D-galactopyranoside (71)**

To a solution of **70** (0.529 g, 0.859 mmol) in MeOH (29 mL) was added NaOMe (192 mg, 3.55 mmol) and stirred for 5 h at room temperature. After neutralization with Amberlite-$H^+$ IR-200 the reaction mixture was filtered and concentrated *in vacuo*. Purification by silica chromatography (50% EtOAc in pentane) resulted in compound **71** (0.369 g, 0.72 mmol, 84%) as a white solid. $[\alpha]D^{20}$ = +21.6 (*c* = 1.0, $CHCl_3$). $^1H$ NMR (400 MHz, $CDCl_3$): δ = 7.56 – 7.49 (m, 2H), 7.48 – 7.21 (m, 8H), 5.44 (s, 1H), 4.75 (s, 2H), 4.32 – 4.24 (m, 2H), 4.11 (d, *J* = 3.4 Hz, 1H), 4.04 – 3.96 (m, 3H), 3.54 – 3.43 (m, 2H), 3.32 (s, 1H), 3.23 (t, *J* = 6.9 Hz, 2H), 2.57 (s, 1H), 1.69 – 1.52 (m, 4H), 1.38 – 1.23 (m, 8H). $^{13}C$ NMR (101 MHz, $CDCl_3$): δ = 138.2, 137.8, 128.9, 128.5, 128.1, 127.9, 126.4, 102.9, 101.1, 79.1, 73.2, 71.5, 70.1, 69.7, 69.3, 66.6, 51.5, 29.5, 29.3, 29.1, 28.8, 26.6, 25.9. HRMS: calculated for $[C_{28}H_{38}N_3O_6]^+$ 512.27551; found 512.27551.

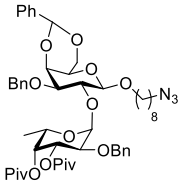

**8-azidooctane 2-*O*-benzyl-3,4-*O*-pivaloyl-α-L-fucopyranosyl (1→2)-3-*O*-benzyl-4,6-*O*-benzylidene-β-D-galactopyranoside (72)**

Compound **71** (0.316 g, 0.618 mmol) and 2-*O*-benzyl-3,4-*O*-pivaloyl-1-thio-α-L-fucopyranoside[32] (0.477 g, 0.928 mmol) were dissolved in $CH_2Cl_2$ (10.3 mL), after which activated molecular sieves (3 Å) and *N*-iodosuccinimide (0.333 g, 1.48 mmol) were added. The reaction mixture was cooled to -45 °C and TMSOTf (11.2 µL, 62 µmol) was added. After stirring for 1 h at -40 °C the reaction mixture was warmed to -15 °C, quenched with $Et_3N$ (3 mL) and washed with $Na_sS_2O_3$ and aqueous saturated $NaHCO_3$. The organic layer was dried with $MgSO_4$, filtered and concentrated *in vacuo*. Purification by column chromatography (20% EtOAc in pentane) gave disaccharide **72** as a white solid (393 mg, 429 µmol, 69%). $[\alpha]D^{20}$ = -36 (*c* = 0.4, $CHCl_3$). $^1H$ NMR (400 MHz, $CDCl_3$): δ = 7.53 (d, *J* = 6.3 Hz, 2H), 7.34 - 7.14 (m, 11H), 7.07 – 7.01 (m, 2H), 5.64 (d, *J* = 3.4 Hz, 1H), 5.43 (s, 2H), 5.40 – 5.34 (m, 1H), 5.24 (d, *J* = 2.4 Hz, 1H), 4.77 – 4.73 (m, 2H), 4.60 (d, *J* = 12.4 Hz, 1H), 4.52 (d, *J* = 11.7 Hz, 1H), 4.46 (d, *J* = 7.8 Hz, 1H), 4.40 (d, *J* = 12.4 Hz, 1H), 4.29 (d, *J* = 12.1 Hz, 1H), 4.22 – 4.13 (m, 2H), 4.02 (d, *J* = 11.8 Hz, 1H), 3.97 – 3.90 (m, 1H), 3.85 – 3.74 (m, 2H), 3.46 – 3.39 (m, 1H), 3.35 (s, 1H), 3.23 (t, *J* = 7.0 Hz, 2H), 1.36 – 1.30 (m, 4H), 1.36 – 1.30 (m, 8H), 1.14 (s, 9H), 1.13 (s, 9H), 1.04 (d, *J* = 6.4 Hz, 3H). $^{13}C$ NMR (101 MHz, $CDCl_3$): δ = 177.8, 177.4, 138.2, 137.8, 137.5, 128.8, 128.5, 128.4, 128.1, 128.0, 127.8, 127.7, 127.6, 127.2, 126.2, 101.6, 100.6, 96.8, 81.3, 72.3, 72.3, 72.0, 71.5, 70.0, 71.4, 70.38, 69.7, 69.3, 66.3, 64.7, 51.4, 39.0, 38.7, 29.6, 29.4, 29.1, 28.8, 27.3, 27.2, 26.7, 26.1, 15.8. HRMS: calculated for $[C_{51}H_{69}N_3O_{12}Na]^+$ 938.47735; found 938.47678.

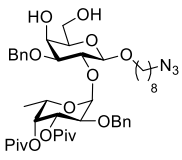

**8-azidooctane 2-*O*-benzyl-3,4-*O*-pivaloyl-α-L-fucopyranosyl (1→2)-3-*O*-benzyl-β-D-galactopyranoside (73)**

Disaccharide **72** (274 mg, 0.300 mmol) was dissolved in AcOH/$H_2O$ (6 mL, 4:1, v/v) and heated to 50 °C. After stirring overnight the reaction mixture was concentrated and co-evaporated with toluene (7x). Purification by silica chromatography (50% EtOAC in pentane) resulted in diol **73** (176 mg, 0.213 mmol, 71%) as a clear oil. $[\alpha]D^{20}$ = -60 (*c* = 1, $CHCl_3$). $^1H$ NMR (400 MHz, $CDCl_3$): δ = 7.38 – 7.23 (m, 5H), 7.23 – 7.13 (m, 3H), 7.09 (dd, *J* = 7.2, 1.9 Hz, 2H), 5.58 (d, *J* = 3.5 Hz, 1H), 5.39 (dd, *J* = 10.8, 3.1 Hz, 1H), 5.26 (d, *J* =

2.4 Hz, 1H), 4.72 – 4.62 (m, 2H), 4.62 – 4.48 (m, 3H), 4.46 (d, *J* = 7.8 Hz, 1H), 4.04 – 3.87 (m, 4H), 3.87 – 3.77 (m, 2H), 3.73 (dd, *J* = 9.3, 3.3 Hz, 1H), 3.52 – 3.46 (m, 2H), 3.26 (t, *J* = 7.0 Hz, 2H), 1.63 – 1.53 (m, 4H), 1.38 – 1.26 (m, 8H), 1.18 (s, 9H), 1.15 (s, 9H), 1.04 (d, *J* = 6.5 Hz, 3H). $^{13}$C NMR (101 MHz, $CDCl_3$): δ = 177.4, 177.4, 137.5, 137.4, 128.7, 128.3, 128.0, 127.8, 127.7, 127.1, 101.8, 97.1, 82.8, 73.8, 72.6, 72.4, 72.3, 71.4, 71.3, 70.2, 70.1, 66.3, 64.9, 62.5, 51.5, 39.0, 38.7, 29.7, 29.4, 29.1, 28.8, 27.2, 27.2, 26.7, 26.0, 15.7. HRMS: calculated for $[C_{44}H_{65}N_3O_{12}Na]^+$ 850.44605; found 850.44555.

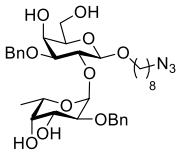

**8-azidooctane 2-*O*-benzyl-α-L-fucopyranosyl (1→2)-3-*O*-benzyl-β-D-galactopyranoside (74)**

Diol **73** (364 mg, 0.44 mmol) was dissolved in a mixture of THF/MeOH/$H_2O$ (44 mL, 5:5:1, v/v/v). After addition of LiOH (197 mg, 8.23 mmol) was heated to 50 °C and stirred for 48 h. The reaction mixture was concentrated *in vacuo* and co-evaporated with toluene (3x). Purification by silica chromatography (100% EtOAC → 10% MeOH in EtOAc) resulted in compound **74** (267 mg, 0.40 mmol, 92%) as a clear oil. $[\alpha]D^{20}$ = -62.4 (*c* = 0.5, $CHCl_3$). $^1$H NMR (400 MHz, $CDCl_3$): δ = 7.35 – 7.22 (m, 8H), 7.14 (dd, *J* = 6.9, 2.6 Hz, 2H), 5.63 (d, *J* = 3.6 Hz, 1H), 4.75 (d, *J* = 11.6 Hz, 1H), 4.64 (d, *J* = 12.0 Hz, 1H), 4.55 – 4.48 (m, 2H), 4.45 (d, *J* = 7.8 Hz, 1H), 4.27 (d, *J* = 12.0 Hz, 1H), 4.11 – 4.07 (m, 1H), 4.06 – 3.94 (m, 3H), 3.93 – 3.88 (m, 1H), 3.87 – 3.82 (m, 1H), 3.79 – 3.75 (m, 1H), 3.73 (dd, *J* = 9.3, 3.3 Hz, 1H), 3.63 (dd, *J* = 9.9, 3.6 Hz, 1H), 3.55 – 3.50 (m, 1H), 3.49 – 3.42 (m, 1H), 3.26 (t, *J* = 6.9 Hz, 2H), 2.50 (s, 1H), 2.36 (s, 1H), 2.22 (s, 1H), 1.62 – 1.54 (m, 4H), 1.32 – 1.22 (m, 11H). $^{13}$C NMR (101 MHz, $CDCl_3$): δ = 137.8, 137.4, 128.8, 128.6, 128.1, 127.9, 127.1, 102.0, 96.2, 83.2, 75.7, 73.9, 72.3, 71.9, 69.5, 71.8, 71.1, 70.0, 66.2, 65.5, 62.5, 51.5, 29.8, 29.5, 29.2, 28.9, 26.8, 26.2, 16.1. HRMS: calculated for $[C_{34}H_{49}N_3O_{10}Na]^+$ 682.33102; found 682.33054.

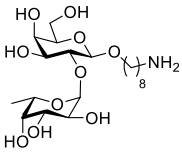

**8-aminooctane α-L-fucopyranosyl (1→2)-β-D-galactopyranoside (75)**

To a solution of compound **74** (59 mg, 89 μmol) in a mixture of THF/$^t$BuOH/$H_2O$ (1:1:3, v/v/v, 2 mL) was added $Pd(OH)_2$/C (100 mg). The reaction mixture was purged with $H_2$ (g). After vigorous stirring overnight, the reaction mixture was filtered and concentrated *in vacuo* resulting in compound **75** (60.5 mg, 67 μmol, 75%) a clear oil. $^1$H NMR (400 MHz, MeOD): δ = 5.22 (s, 1H), 4.34 – 4.23 (m, 2H), 3.96 – 3.90 (m, 1H), 3.88 – 3.83 (m, 1H), 3.80 – 3.62 (m, 4H), 3.59 – 3.45 (m, 2H), 2.91 – 2.87 (m, 2H), 1.66 (m, 4H), 1.45 – 1.30 (m, 8H), 1.21 (d, *J* = 6.4 Hz, 3H). $^{13}$C NMR (101 MHz, MeOD): δ = 103.6, 101.5, 79.0, 76.4, 75.6, 73.7, 71.7, 70.7, 70.6, 70.4, 67.8, 62.4, 49.6, 49.4, 49.2, 49.0, 48.8, 48.6, 48.4, 40.8, 30.9, 30.2, 30.1, 28.5, 27.3, 27.1, 16.8.

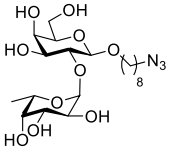

**8-azidooctane α-L-fucopyranosyl (1→2)-β-D-galactopyranoside (63)**

Amine **75** (28.1 mg, 61.9 μmol) was dissolved in MeOH/$H_2O$ (2 mL, 1:1, v/v) and $K_2CO_3$ (25.6 mg, 0.186 mmol) and $CuSO_4.5H_2O$ (1.2 mg) were added. After addition of imidazole-1-sulfonyl azide.HCl (20 mg, 0.93 mmol) the reaction was stirred overnight. The reaction mixture was concentrated *in vacuo*, co-evapporated with toluene (3x) and redissolved in pyridine (6.2 mL). After addition of $Ac_2O$ (1.0 mL, 10.6 mmol) the reaction mixture was stirred for 48 h. The reaction mixture was concentrated *in vacuo*

and purificated by silica chromatography (30% EtOAc in pentane). $^1$H NMR (400 MHz, $CDCl_3$): δ = 5.39 (d, *J* = 3.9 Hz, 1H), 5.34 – 5.26 (m, 3H), 5.06 – 4.93 (m, 2H), 4.60 (dd, *J* = 4.0, 13.0 Hz, 1H), 4.46 (d, *J* = 7.8 Hz, 1H), 4.19 (dd, *J* = 11.2, 6.4 Hz, 1H), 4.10 (dd, *J* = 11.2, 7.1 Hz, 1H), 3.99 – 3.83 (m, 3H), 3.57 – 3.48 (m, 1H), 3.27 (t, *J* = 7.0 Hz, 2H), 2.16 (s, 3H), 2.13 (s, 3H), 2.05 (s, 3H), 2.01 (s, 3H), 1.99 (s, 3H), 1.98 (s, 3H), 1.67 – 1.55 (m, 4H), 1.42 – 1.31 (m, 8H), 1.12 (d, *J* = 6.5 Hz, 3H). $^{13}$C NMR (101 MHz, $CDCl_3$): δ = 170.8, 170.5, 101.7, 95.8, 77.5, 77.2, 76.8, 73.9, 71.78, 71.3, 70.5, 70.4, 68.4, 67.8, 67.3, 64.7, 61.3, 51.6, 29.7, 29.4, 29.2, 28.9, 26.8, 26.1, 20.8, 20.8, 15.9. Next, the residue was dissolved in MeOH (4 mL) and NaOMe (catalytic amount) was added. After stirring for 30 min, the reaction mixture was neutralized with Amberlite-$H^+$ IR-200, filtrated and concentrated *in vacuo* to obtain target compound **63** (8.3 mg, 17.3 µmol, 28% over three steps) as a white solid. $^1$H NMR (400 MHz, MeOD): δ = 5.20 (s, 1H), 4.34 – 4.26 (m, 2H), 3.91 (m, *J* = 9.4, 6.7 Hz, 1H), 3.82 (d, *J* = 2.4 Hz, 1H), 3.78 – 3.70 (m, 4H), 3.70 – 3.63 (m, 3H), 3.57 – 3.47 (m, 2H), 3.28 (t, *J* = 8.0 Hz, 2H), 1.66 – 1.54 (m, 4H), 1.43 – 1.31 (m, 8H), 1.19 (d, *J* = 6.6 Hz, 3H). $^{13}$C NMR (101 MHz, MeOD): δ = 103.6, 101.6, 79.0, 76.5, 75.8, 73.8, 71.8, 70.7, 70.6, 70.4, 67.8, 62.4, 52.4, 49.6, 49.4, 49.2, 49.0, 48.8, 48.6, 48.4, 31.0, 30.5, 30.3, 29.9, 27.8, 27.2, 16.8. HRMS: calculated for $[C_{20}H_{37}N_3O_{10}Na]^+$ 502.23712; found 502.23683.

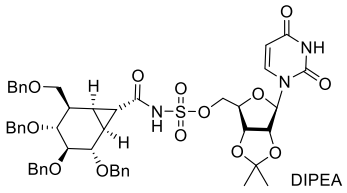


**DIPEA salt of ((3a*R*,4*R*,6*R*,6a*R*)-6-(2,4-dioxo-3,4-dihydropyrimidin-1(2H)-yl)-2,2-dimethyltetrahydrofuro[3,4-d][1,3]dioxol-4-yl)methyl ((1*R*,2*S*,3*R*,4*R*,5*R*,6*R*,7*R*)-2,3,4-tris(benzyloxy)-5-((benzyloxy)methyl)bicyclo[4.1.0]heptane-7-carbonyl)sulfamate (67)**

To a solution of carboxylic acid **66**[33] (60 mg, 0.10 mmol) in toluene (6.0 mL) was added oxalyl chloride (1 M in DCM, 0.30 mL, 0.30 mmol, 3.0 eq.). After stirring for 5 at reflux conditions, the reaction mixture was concentrated *in vacuo* and redissolved in DCM (7.0 mL). 2',3'-*O*-Isopropylidene-5'-*O*-sulfamoyluridine[34] (0.100 g, 0.27 mmol, 2.3 eq.) and DIPEA (40 µL, 0.24 mmol, 2.4 eq.) were added. After stirring overnight at room temperature, the reaction mixture was concentrated under reduced pressure and purified by size exclusion column chromatography (DCM/MeOH, 1:1), resulting in sulfonamide **67** (90 mg, 86 µmol, 86%) as a white wax. $^1$H NMR (400 MHz, MeOD): δ (ppm) 7.76 (d, J = 7.6 Hz, 1H), 7.38 – 7.17 (m, 20H), 5.94 – 5.88 (m, 1H), 5.72 (d, J = 6.4 Hz, 1H), 4.87 (d, J = 1.9 Hz, 2H), 4.84 – 4.67 (m, 4H), 4.62 – 4.54 (m, 2H), 4.52 – 4.43 (m, 2H), 4.41 – 4.35 (m, 1H), 4.30 – 4.23 (m, 2H), 3.74 (d, J = 5.8 Hz, 1H), 3.70 – 3.66 (m, 3H), 3.67 – 3.64 (m, 1H) 3.54 – 3.42 (m, 2H), 3.21 – 3.14 (m, 2H), 3.10 (t, J = 10.1 Hz, 1H), 2.39 – 2.28 (m, 1H), 1.94 (dd, J = 9.2, 4.7 Hz, 1H), 1.71 (dd, J = 9.1, 4.4 Hz, 1H), 1.61 (t, J = 4.6 Hz, 1H), 1.50 (d, J = 13.9 Hz, 3H), 1.32 (m, 15H). $^{13}$C NMR (101 MHz, MeOD): δ (ppm) 179.1, 166.0, 152.0, 143.7, 143.7, 140.2, 139.9, 139.8, 139.6, 129.5, 129.5, 129.4, 129.3, 129.2, 129.1, 129.1, 128.9, 128.7, 128.7, 128.6, 128.5, 128.5, 115.2, 103.2, 93.7, 87.0, 85.4, 85.3, 82.5, 82.4, 77.7, 76.0, 75.9, 74.2, 72.6, 71.8, 70.2, 55.8, 43.8, 41.9, 27.5, 27.1, 26.5, 26.2, 25.6, 13.2.

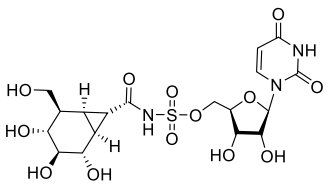

**((2*R*,5*R*)-5-(2,4-dioxo-3,4-dihydropyrimidin-1(2H)-yl)-3,4-dihydroxytetrahydrofuran-2-yl)methyl ((1*R*,2*S*,3*R*,4*R*,5*R*,6*R*,7*R*)-2,3,4-trihydroxy-5-(hydroxymethyl)bicyclo[4.1.0]heptane-7-carbonyl)sulfamate (65, ML131)**

To a solution of sulfonamide **67** (89 mg, 84 µmol) in DCM (10 mL) was drop-wise added $BCl_3$ (1 M in DCM, 1.15 mL, 1.15 mmol, 13.7 eq.) at 0 °C. After stirring for 3 h, the reaction mixture was quenched with MeOH and stirred for 30 min. The reaction mixture was concentrated *in vacuo*, redissolved in $CHCl_3$ and stirred vigorously for 30 min before the suspension was filtered. The residue was taken up in methanol, concentrated *in vacuo* and purificated by HPLC (C18 column, linear gradient: 5 → 10% B in A, solutions used A: $H_2O$, B: acetonitrile, 0.5% TFA, 15 min) to obtain compound **65** (8.6 mg, 16 µmol, 20%) as a white solid. $^1$H NMR (400 MHz, $CDCl_3$): δ 7.73 (d, J = 8.2 Hz, 1H), 5.90 (d, J = 4.5 Hz, 1H), 5.75 (d, J = 8.1 Hz, 1H), 4.55 – 4.48 (m, 2H), 4.20 (dd, J = 4.9, 2.5 Hz, 1H), 4.13 (dd, J = 7.0, 4.7 Hz, 2H), 3.96 – 3.92 (m, 1H), 3.57 (d, J = 8.3 Hz, 1H), 3.19 (dd, J = 10.0, 8.3 Hz, 1H), 2.89 (t, J = 10.1 Hz, 1H), 2.16 (s, 1H), 2.03 – 1.97 (m, 1H), 1.58 (s, 1H). $^{13}$C NMR (101 MHz, $CDCl_3$): δ 172.8, 152.4, 142.4, 103.1, 90.7, 82.7, 79.3, 75.0, 74.0, 72.2, 71.0, 69.7, 64.2, 43.7, 30.2, 28.0, 24.3. HRMS: calculated for $[C_{18}H_{26}N_3O_{13}S]^+$ 524.11808, found 524.11799.

**Materials of biological assays**

Recombinant human GBA1 (Cerezyme), recombinant human GAA (Myozyme) and recombinant human α-Gal A (Fabrazyme) were obtained from Genzyme, USA. Cellular homogenates of a stable human embryonic kidney 293 (HEK293) over-expressing GBA2 cell line[35] were pre-incubated for 30 min with an inhibitor of GBA1 (1 mM conduritol B epoxide (CBE)). Galactocerebrosidase (GALC) was obtained by expressing recombinant murine GALC in HEK293 cells after which the secreted recombinant protein in the culture medium was directly used.[36] Fibroblasts of Pompe patients diagnosed on the basis of reduced GAA activity (obtained with consent from donors) were used for GANAB determinations.

**Enzyme activity assays, determination of the apparent $IC_{50}$ values**

All activity assays were performed at 37 °C. To determine the apparent $IC_{50}$ values, enzyme preparations were pre-incubated with a range of inhibitor concentrations for 30 min, where after the residual activity was measured by addition of the appropriated 4-methylumbelliferyl-based substrate mix. GBA1 residual activity was measured with 3.7 mM 4-methylumbeliferone(4-mu)-β-D-glucopyranoside in 150 mM McIlvaine buffer, pH 5.2, supplemented with 0.2% Taurocholate (w/v), 0.1% Triton X-100 (v/v), 0.1% Bovine Serum albumin (BSA) (w/v) for 30 min. GBA2 substrate mix consisted of 3.7 mM 4-mu-β-D-glucopyranoside in 150 mM McIlvaine, pH 5.8, 0.1% BSA (w/v) and was incubated for 1 h. α-Gal A activity was determined with 2 mM 4-mu-α-D-galactopyranoside dissolved in 150 mM McIlvaine, pH 4.5, 0.1% BSA (w/v) for 30 min. GAA substrate mix consisted of 3 mM 4-mu-α-D-glucopyranoside pH 5.0, 0.1% BSA (w/v) for 1 h, GALC was assayed with 1.25 mM 4-mu-β-D-galactopyranoside in 150 mM McIlvaine pH 4.3 containing 0.2 M NaCl and 0.1% BSA (w/v) for 1h and GANAB with 3 mM 4-mu-α-D-glucopyranoside pH 7.0, 0.1% BSA (w/v) for 2 h. After stopping the substrate reaction with an excess of 1 M NaOH-glycine (pH 10.3), liberated 4-mu

fluorescence was measured with a fluorimeter LS55 (Perkin Elmer) using $\lambda_{Ex}$ 366 nm and $\lambda_{Em}$ 445 nm. All $IC_{50}$ values were determined in triplicate with Graphpad Prism 5 software.

## References


(1) Willems, L. I.; Beenakker, T. J. M.; Murray, B.; Gagestein, B.; van den Elst, H.; van Rijssel, E. R.; Codée, J. D. C.; Kallemeijn, W. W.; Aerts, J. M. F. G.; van der Marel, G. A.; Overkleeft, H. S. *Eur. J. Org. Chem.* **2014**, *2014*, 6044.

(2) Olszewska, E.; Borzym-Kluczyk, M.; Rzewnicki, I.; Wojtowicz, J.; Rogowski, M.; Pietruski, J. K.; Czajkowska, A.; Sieskiewicz, A. *Współczesna Onkol.* **2012**, *2*, 154.

(3) Speciale, G.; Thompson, A. J.; Davies, G. J.; Williams, S. J. *Curr. Opin. Struc. Biol.* **2014**, *28*, 1.

(4) Maita, N.; Tsukimura, T.; Taniguchi, T.; Saito, S.; Ohno, K.; Taniguchi, H.; Sakuraba, H. *Proc. Natl. Acad. Sci. USA* **2013**, *110*, 14628.

(5) Bie, H.; Yin, J.; He, X.; Kermode, A. R.; Goddard-Borger, E. D.; Withers, S. G.; James, M. N. G. *Nat. Chem. Biol.* **2013**, *9*, 739.

(6) Lagaert, S.; Pollet, A.; Delcour, J. A.; Lavigne, R.; Courtin, C. M.; Volckaert, G. *Appl. Microbiol. Biotechnol.* **2011**, *92*, 1179.

(7) Yadav, V.; Yadav, P. K.; Yadav, S.; Yadav, K. D. S. *Process Biochem.* **2010**, *45*, 1226.

(8) Zverlov, V. V.; Hertel, C.; Bronnenmeier, K.; Hroch, A.; Kellermann, J.; Schwarz, W. H. *Mol. Microbiol.* **2000**, *35*, 173.

(9) O'Neill, E. C.; Stevenson, C. E. M.; Paterson, M. J.; Rejzek, M.; Chauvin, A.-L.; Lawson, D. M.; Field, R. A. *Proteins* **2015**, *83*, 1742.

(10) Hansen, F. G.; Bundgaard, E.; Madsen, R. *J. Org. Chem.* **2005**, *70*, 10139.

(11) Li, K.-Y.; Jiang, J.; Witte, M. D.; Kallemeijn, W. W.; van den Elst, H.; Wong, C.-S.; Chander, S. D.; Hoogendoorn, S.; Beenakker, T. J. M.; Codée, J. D. C.; Aerts, J. M. F. G.; van der Marel, G. A.; Overkleeft, H. S. *Eur. J. Org. Chem.* **2014**, *2014*, 6030.

(12) Yun, M.; Moon, H. R.; Kim, H. O.; Choi, W. J.; Kim, Y.-C.; Park, C.-S.; Jeong, L. S. *Tetrahedron Lett.* **2005**, *46*, 5903.

(13) Jiang, J.; Kallemeijn, W. W.; Wright, D. W.; van den Nieuwendijk, A. M. C. H.; Rohde, V. C.; Folch, E. C.; van den Elst, H.; Florea, B. I.; Scheij, S.; Donker-Koopman, W. E.; Verhoek, M.; Li, N.; Schürmann, M.; Mink, D.; Boot, R. G.; Codée, J. D. C.; van der Marel, G. A.; Davies, G. J.; Aerts, J. M. F. G.; Overkleeft, H. S. *Chem. Sci.* **2015**, *6*, 2782.

(14) Serrano, P.; Llebaria, A.; Vázquez, J.; de Pablo, J.; Anglada, J. M.; Delgado, A. *Chem. Eur. J.* **2005**, *11*, 4465.

(15) Shing, T.; Tam, E. *Tetrahedron Lett.* **1999**, *40*, 2179.

(16) Gloster, T. M.; Davies, G. J. *Org. Biomol. Chem.* **2010**, *8*, 305.

(17) Platt, F. M.; Neises, G. R.; Dwek, R. A.; Butters, T. D. *J. Biol. Chem.* **1994**.

(18) Ficicioglu, C. *Ther Clin Risk Manag* **2008**, *4*, 425.

(19) Aerts, J. M.; Hollak, C.; Boot, R.; Groener, A. *Philos. Trans. R. Soc. London. Ser B* **2003**, *358*, 905.

(20) Wennekes, T.; van den Berg, R. J. B. H. N.; Donker, W.; van der Marel, G. A.; Strijland, A.; Aerts, J. M. F. G.; Overkleeft, H. S. *J. Org. Chem.* **2007**, *72*, 1088.

(21) van den Berg, R. J. B. H. N.; van Rijssel, E. R.; Ferraz, M. J.; Houben, J.; Strijland, A.; Donker-Koopman, W. E.; Wennekes, T.; Bonger, K. M.; Ghisaidoobe, A. B. T.; Hoogendoorn, S.; van der Marel, G. A.; Codée, J. D. C.; Overkleeft, H. S.; Aerts, J. M. F. G. *ChemMedChem* **2015**, *10*, 2042.

(22) Lopez, O. L.; Fernández-Bolaños, J. G.; Lillelund, V. H.; Bols, M. *Org. Biomol. Chem.* **2003**, *1*, 478.

(23) Ovaa, H.; Lastdrager, B.; Codée, J. D. C.; van der Marel, G. A.; Overkleeft, H. S.; van Boom, J. H. *J. Chem. Soc., Perkin Trans. 1* **2002**, *42*, 2370.

(24) Hyldtoft, L.; Madsen, R. *J. Am. Chem. Soc.* **2000**, *122*, 8444.

(25) Pesnot, T.; Jørgensen, R.; Palcic, M. M.; Wagner, G. K. *Nat. Chem. Biol.* **2010**, *6*, 321.

(26) Filippov, D.; Kuyl-Yeheskiely, E.; van der Marel, G. A.; Tesser, G. I.; van Boom, J. H. *Tetrahedron Lett.* **1998**, *39*, 3597.

(27) Watkins, W. M. *Pure Appl. Chem.* **1991**, *63*, 561.

(28) Persson, M.; Palcic, M. M. *Anal. Biochem.* **2008**, *378*, 1.

(29) Deng, S.; Yu, B.; Guo, Z.; Hui, Y. *J. Carbohyd. Chem.* **1998**, *17*, 439.

(30) Fernandez-Mayoralas, A.; Marra, A.; Trumtel, M.; Veyrières, A.; Sinaÿ, P. *Carbohydr. Res.* **2001**, *188*, 81.

(31) The synthesis of 1-azido-8-iodooctane is described in Chapter 3 of this Thesis.

(32) Akcay, G.; Ramphal, J. Y.; d'Alarcao, M.; Kumar, K. *Tetrahedron Lett.* **2015**, *56*, 109.

(33) The synthesis of carboxylic acid **66** is described in Chapter 8 of this Thesis.

(34) Zhang, G.-L.; Zhang, L.-H.; Ye, X.-S. *Org. Biomol. Chem.* **2010**, *8* (22), 5062.

(35) Marques, A. R. A.; Mirzaian, M.; Akiyama, H.; Wisse, P.; Ferraz, M. J.; Gaspar, P.; Ghauharali-van der Vlugt, K.; Meijer, R.; Giraldo, P.; Alfonso, P.; Irún, P.; Dahl, M.; Karlsson, S.; Pavlova, E. V.; Cox, T. M.; Scheij, S.; Verhoek, M.; Ottenhoff, R.; van Roomen, C. P. A. A.; Pannu, N. S.; van Eijk, M.; Dekker, N.; Boot, R. G.; Overkleeft, H. S.; Blommaart, E.; Hirabayashi, Y.; Aerts, J. M. *J. Lipid Res.* **2016**, *57*, 451.

(36) Marques, A. R.; Willems, L. I.; Herrera Moro, D.; Florea, B. I.; Scheij, S.; Ottenhoff, R.; van Roomen, C.; Verhoek, M.; Nelson, J. K.; Kallemeijn, W. W.; Biela-Banas, A.; Martin, O. R.; Cachón-González, M. B.; Kim, N. N.; Cox, T. M.; Boot, R. G.; Overkleeft, H. S.; Aerts, J. M. F. G.; A. M. D. G. *Chembiochem* **2017**, *18*, 1.